TURKISH JOURNAL of ONCOLOGY

Turk J Oncol 2020;35(3):298–305
doi: 10.5505/tjo.2020.2264

ORIGINAL ARTICLE

A Different Approach to Intensity Modulated Radiation Therapy Patient QA Measurements about Dosimetric Equipment

Aysun İNAL,[1] İsmail Hakkı SARPÜN,[2] Rıdvan ÜNAL[3]

[1]Department of Radiation Oncology, University of Health Sciences, Antalya Training and Research Hospital, Antalya-*Turkey*
[2]Department of Physics, Akdeniz University, Faculty of Science, Antalya-*Turkey*
[3]Department of Medical Imaging, Uşak University, Vocational School of Health Sciences, Uşak-*Turkey*

OBJECTIVE

In Patient Quality Assurance measurements for Intensity Modulated Radiation Therapy, this study aimed to investigate the dosimetric differences between the calculated and measured values when the standard dosimetric equipment contains the different density materials.

METHODS

In this study, a setup that can be used for both absolute dose and planar dose distribution is considered aimed to investigate the effects of the selected grid size value in the treatment planning system on the Monitor Unit, 2D array gamma evaluation and absorbed dose measurements. Also, the effects of using different "distance to agreement" values and the effects of using cylindrical/inhomogeneous phantom instead of square/homogeneous on 2D array gamma evaluation and absorbed dose measurements were investigated.

RESULTS

The considerable difference between the calculated dose and measured dose for grid size 0.1 cm was found to be 2.96% for the square/homogeneous phantom and 5.75% for the cylindrical/inhomogeneous phantom. According to the 3%/2 mm criterion, Setup1 allowed treatment with 98.76%, whereas this value was below our acceptance limit with 88.39% for Setup 2.

CONCLUSION

In addition to the standard IMRT patient QA procedure, we are of the opinion that the use of clinically different dosimetric equipment provides an idea of the control of different grid size values of TPS calculation algorithms.

Keywords: IMRT; inhomogeneity; gamma evaluation; patient QA.

Introduction

Radiation Therapy plays an important role in cancer treatment. The treatment techniques, such as Intensity Modulated Radiation Therapy (IMRT), Volumetric Arc Therapy (VMAT) and Stereotactic Radiation Therapy (SRS), with advancing technology, enable complex dose distribution around target volume with minimal damage to normal tissues.[1] These techniques require a series of irradiation fields of varying

Received: February 26, 2020
Accepted: February 29, 2020
Online: April 13, 2020

Accessible online at:
www.onkder.org

Dr. Aysun İNAL
Antalya Eğitim ve Araştırma Hastanesi,
Sağlık Bilimleri Üniversitesi,
Radyasyon Onkolojisi Kliniği,
Antalya-Turkey
E-mail: aysuntoy@yahoo.com

intensity for implementing the prescribed dose to the target volume.[2-8]

The major challenges with the advancement of technology in transitioning from three-dimensional conformal therapy to IMRT are the lack of error data with the new treatment techniques and the loss of applicability of traditionally used methods and dosimetric equipment. For example, in addition to the point dose measurements used in conformal treatment, the two-dimensional dose mapping has been added.[9,10]

In this context, the European Society for Radiotherapy & Oncology (ESTRO) has launched a network of Quality Assurance of Intensity Modulated Radiation Oncology (QUASIMOD) among fifteen European centers.[11] In the Task Group 119 report published by the American Association of Physicists in Medicine (AAPM), point-dose measurement and planar dose verification are safe for IMRT application.[12] The reason for this is that the radiation dose planned before treatment in IMRT should be fully confirmed.[13]

The improvements in IMRT procedures have had a significant impact on both the clinical and physical development of radiotherapy. Quality Assurance (QA) procedures and the clinical requirements of IMRT have been the driving force behind many medical physics research activities.

There are several dosimetry systems, such as ionization chambers, GafChromic films and two-dimensional (2D) arrays, which can be used for quality assurance before patient treatment. Ionization chambers are used to compare absorbed doses calculated in the treatment planning system to the measured on the treatment machine.[14] The GafChromic film confirms the planar dose by 3D irradiation, making the same arrangement in clinical treatments. Van Esch et al. reported that the time they spend for all these procedures is 3-10 hours per patient.[15] Thus, the film dosimeter has been relocated gradually with 2D multiple detectors for pretreatment verification of patient-specific IMRT dose distribution because of its ease of use and immediate evaluation of the results,[13] which requires much less time than is required to perform a similar analysis with GafChromic film. The 2D diode array is ideal for quality assurance per plan after an IMRT system is fully commissioned.[16]

The human body has many non-homogeneous structures and does not have a square and/or rectangular structure as modeled in studies, such as a 2D array and/or solid phantoms. In addition, separate measurements of absorbed dose by ion chamber and dose distribution map by 2D array lead to time loss.

In treatment planning systems (TPS), uncertainties in dose calculation are a result of dose and position errors when the dose calculation is interpolated linearly between grid points. Niemierko and Goitien have shown that the magnitude of dose and position errors depends on the width of the beam penumbra.[17] Although a smaller grid size can give us a more accurate and consistent dose calculation in size, especially in high dose gradient regions, a finer calculation requires a longer calculation time than dose calculations using grid size.[17,18] Several studies have been conducted looking at the grid size for different treatment fields and techniques. Dempsey et al. found that the 0.25 cm grid size range was sufficient to reduce the dose calculation error in IMRT to less than 1% using Fourier analysis.[19] Variable grid size with 0.2-0.4 cm differences was found to cause a 2-4% dose mismatch for head and neck IMRT.[20] The optimal grid size was found to be 0.3 cm in lung stereotactic therapies using dynamic arc therapy.[21] While there are many studies for the grid size for the calculation of patient plans, there is no clear answer for the selection of grid size to be used in calculations for patient QA plan before treatment. In patient QA processes, tools, such as film, 2D array and ion chamber, are used. In these measurements, we think that the effect of grid size is more important in the results obtained with the 2D array. The reason we think this may be important is that because the distance of the ion chambers in the 2D array systems is larger, which requires interpolation between points.

The gamma evaluation (γ) is the examination of the plan according to both successful and unsuccessful criteria for dose distribution comparisons on the base of both dose difference (DD) and distance to agreement (DTA). The criterion of success is that the gamma value is equal to and/or less than 1.[22] During gamma evaluation, the dose change for the distance between the two selected points is checked. Even though the dose difference of 3% criterion is set to be the standard for the dose difference, it becomes important to choose the dose between two points in the selection of DTA.[13]

The main reason for that is DTA's sensitivity in low dose gradient regions. For plan acceptance, the percentage value of the rate that meets this criterion may vary depending on the intra-clinical decision. Pulliam et al. reported QA results for 13.000 patients receiving IMRT in their clinics that the most point dose differences were within ±3% of tolerance, whereas failed plans were only a few % beyond tolerance.[23] Furthermore, in gamma evaluations, the initiation criterion of IMRT in their institution was 90% of the pixels that exceeded the 5%/3

Turk J Oncol 2020;35(3):298–305
doi: 10.5505/tjo.2020.2264

mm criterion without the low dose threshold.[23] In our clinic, the acceptance criterion was determined as 98.5% of the pixels exceeding 3%/3 mm criteria.

In this study, a setup that can be used for both absolute dose and planar dose distribution is considered aimed to answer the following questions:

1. What is the effect of the calculation grid size value selected in the TPS on the Monitor Unit (MU)?
2. What is the effect of the selected grid size value in the TPS on 2D array gamma evaluation and absorbed dose measurements?
3. What is the effect of using different DTA values on gamma result in 2D array measurements?
4. What is the effect of using cylindrical/inhomogeneous (C/I) phantom instead of square/homogeneous (S/H) on 2D array gamma evaluation and absorbed dose measurements?

Materials and Methods

Preparation of Phantoms and CT Examination

Two different phantom assemblies schematically illustrated in Figure 1. In both embodiments, the CC04 (IBA Dosimetry GmbH, Germany) model ionization chamber with an active volume of 0.04 cc on the 2D array (I'mRTMatriXX of ScanditronixWellhofer, Germany), consisting of 1020 (detectors with an active volume of 0.08 cc in diameter and a distance between the detectors of 7.62 mm and a diameter of 4.5 mm, can measure 2D dose map array which is called MatriXX.

In the first embodiment, there are 20 water-equivalent solid phantoms (SP34 white polystyrene IBA Dosimetry GmbH, Germany) for S/H, and each size is 30cmx30cm x1cm (Setup 1). In the second embodiment, instead of all S/H water-equivalent phantoms over the ion chamber, a cylindrical/inhomogeneous phantom of a 20 cm diameter, which includes nine materials of different density (Setup 2) was placed (By Truck The phantom laboratory, Greenwich, NY).

In both phantom assemblies, General Electric (GE) brand (GE-Light Speed 64, GE, USA) Computed Tomography (CT) device, axial cross-section, taken slices were sent to ElektaXiO (CMS Co., Ltd, St Louis, MO, USA) treatment planning system.

Procedures in TPS

The phantom frame is contoured at TPS on transverse sections of two different assemblies from CT. A 7-field IMRT plan with 6 Mega Volt (MV) photon energy of a head and neck patient was calculated for three different grid sizes (0.3, 0.2 and 0.1 mm). All calculations for IMRT patient QA in TPS were performed using the superposition algorithm. Superposition algorithm accounts for scattering component transport in hetero-

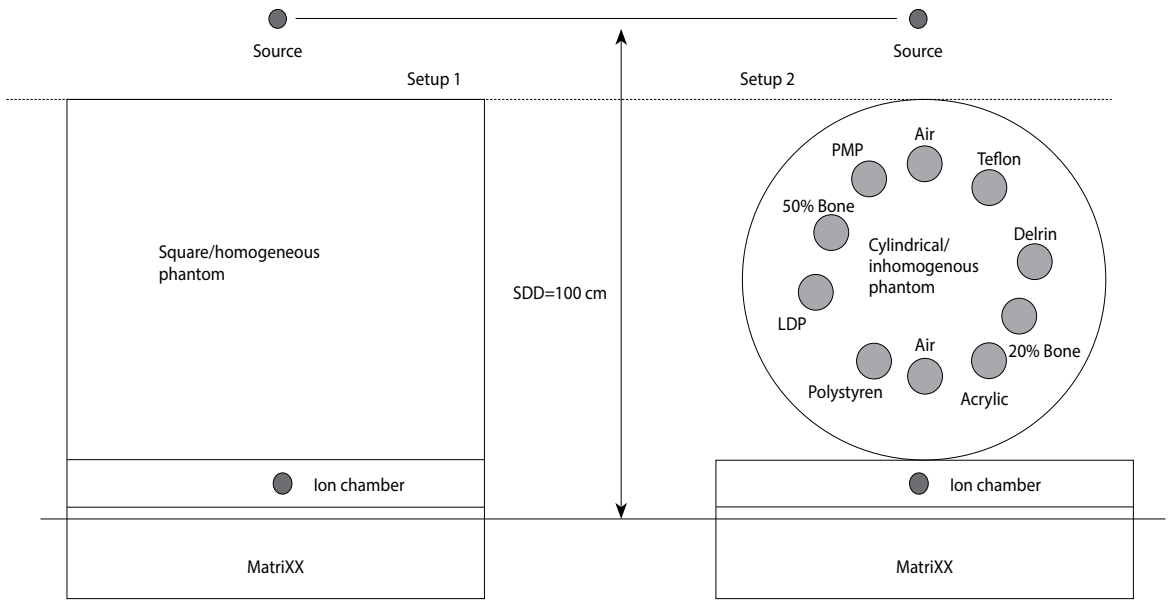

Fig. 1. Schematic representation of the phantom assemblies prepared for Setup 1 and Setup 2.
SDD: Source detector distance

geneous media. Kernels were modified with a relative electron density of the media. Also, the step and shoot optimization techniques were used.

When calculating dose and MU data, Q1 (Q1=Field 1) is the first field irradiation. Consecutive fields are expressed as the sum of the dose values. For example; the second field is Q2=Q1+Field2, while the last field is calculated as the sum of all fields Q6+Field 7 (Q7). At the same time, the dose administered per field is taken as the reference for 0.2 cm grid size and the MUs corresponding to this dose in the other grid sizes are calculated according to the same formulation.

For MatriXX measurements, the 2D plane dose maps at the point where the detectors are located were calculated for each grid size and both phantom assemblies. The calculated and measured values were compared by Gamma Evaluation Method.

Procedures on Linear Accelerator Measurements

Before starting the measurements, the Linear Accelerator (Elekta Synergy Platform, Elekta, Crawley, UK) was calibrated at a maximum dose point of 6 MV, equivalent to 1 cGy to 1 MU on 10x10 cm^2 field size and 100 cm source-surface distance.

The phantoms are positioned in the geometry and position placed on the CT on the treatment table. In order to check the placement of the phantoms and the accuracy of the planned isocenter in the TPS, the Anterior-Posterior and Lateral images of both phantom assemblies were taken before the measurement, and necessary geometric corrections were made.

In both assemblies, readings in the ion chamber were taken with the Dose1 Electrometer (Dose 1 Electrometer, IBA Dosimetry GmbH, Germany). The readings were converted to absorbed dose using calibration factors and temperature-pressure correction.

Source to MatriXX Detector plane distance (SDD) at 100 cm where ion chamber placed 1 cm above detector plane and simultaneous measurements were taken. Measurements were compared with calculated plans made on different grid size. The planar dose map measured in the comparison is converted according to the grid size selected in the planning. In the gamma evaluation, the dose difference was always taken as 3%, while for DTA, 2 mm and 1 mm, two different distances were used.

Results

While the defined dose is constant, the MU values in seven sub-fields for IMRT planning according to grid size change are found for Setup 1 and Setup 2. As shown in Figure 2, Setup 1 defined doses are used as a grid

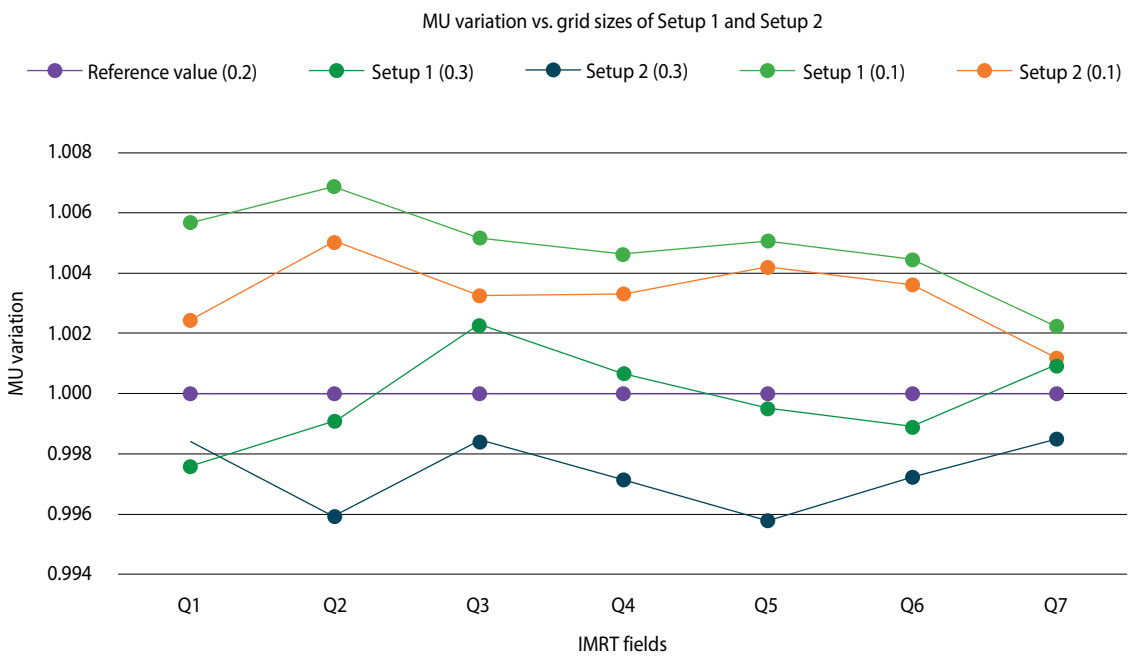

Fig. 2. After a grid size (in this case 0.2 cm) value was set to 1, the other values were normalized accordingly and MU variations were graphed against the Q1 to Q7 IMRT fields for Setup1.

Turk J Oncol 2020;35(3):298–305
doi: 10.5505/tjo.2020.2264

Table 1 In both setups, for all field and grid sizes, the absorbed dose values calculated in the TPS and measured by the ion chamber and the % dose differences between them

Grid size (cm) IMRT fields	0.3	0.2 Setup 1	0.1	0.3	0.2 Setup 2	0.1
CD for Q1	9.60	9.51	9.50	9.50	9.60	9.60
MD for Q1	10.04	10.04	10.04	10.19	10.19	10.19
DD%	4.36	5.26	5.36	6.73	5.75	5.75
CD for Q2	29.20	29.40	29.50	29.80	30.00	30.20
MD for Q2	29.83	29.83	29.83	30.47	30.47	30.47
Difference%	2.10	1.43	1.10	2.20	1.55	0.89
CD for Q3	50.30	50.10	50.20	51.00	51.10	51.30
MD for Q3	51.00	51.00	51.00	52.14	52.14	52.14
DD%	1.39	1.80	1.59	2.24	2.04	1.65
CD for Q4	66.40	65.80	66.00	67.00	66.60	67.00
MD for Q4	66.22	66.22	66.22	67.55	67.55	67.55
DD%	0.27	0.63	0.33	0.82	1.41	0.82
CD for Q5	84.20	83.90	83.50	85.00	84.90	84.70
MD for Q5	85.16	85.16	85.16	86.92	86.92	86.92
DD%	1.13	1.48	1.95	2.21	2.33	2.56
CD for Q6	107.80	107.60	107.30	108.90	109.00	108.90
MD for Q6	108.54	108.54	108.54	110.73	110.73	110.73
DD%	0.68	0.86	1.14	1.65	1.56	1.65
CD for Q7	128.30	128.00	127.50	129.70	129.80	129.50
MD for Q7	129.10	129.10	129.10	131.82	131.82	131.82
DD%	0.62	0.85	1.24	1.61	1.53	1.76

CD: Calculated dose; MD: Measured dose; DD%: Percent dose difference; TPS: Treatment planning system; Q1: Field 1; Q2: Q1+Field 2; Q3: Q2+Field 3; Q4: Q3+ Field 4; Q5: Q4+Field 5; Q6: Q5+Field 6; Q7: Q6+Field 7

size 0.2 cm reference and taken as "1". For all fields, the MUs were normalized to the reference value. According to the results, while Q1, Q2 and Q3 were decreased by grid size, MU increased by Q4, Q5, Q6 and Q7 and vice versa. The largest MU difference was found to be 0.81% (122.8-123.8) and 1.2% (121.9 -123.4) for Setup 1 and Setup 2, respectively, between 0.3 and 0.1 cm. The biggest difference between Setup 1 and Setup 2 was 0.3 cm for the grid size, which corresponds to 0.73% difference.

The absorbed dose measurements taken in the ion chamber and the TPS dose calculations for different grid sizes are shown in Table 1 for Setup 1 and Setup 2. The considerable difference between the calculated dose (CD) and measured dose (MD) for grid size 0.1cm was found to be 2.96% for the square/homogeneous phantom and 5.75% for the cylindrical/inhomogeneous phantom. Although the percentage difference of CD-MD according to the grid size differs for each field, the Q7 total measurement evaluation shows that the best 0.3 cm grid size for square/homogeneous phantom and 0.2 cm grid size for cylindrical/inhomogeneous phantom.

Also, as one can see in Table 1, the difference between the measured and calculated absorbed dose comparisons was found to be higher in the presence of cylindrical/inhomogeneous phantoms. The biggest differences in the Q1 field CD-MD comparison, % dose differences for Setup 1 were found to be 5.36 for 0.1 cm grid size and for Setup 2 were found to be 6.73 for 0.3 cm grid size (Table 1).

The results of gamma evaluation of the measurements taken by MatriXX according to different grid sizes are shown in Table 2 for Setup 1 and Setup 2. In this study, 99.5% gamma value was taken as reference for 3%/3 mm found according to the plan calculated with 0.2 cm. According to the results, gamma evaluation in Setup 1 provided $\gamma \leq 1$condition better than Setup 2 for all grid sizes and DTA values.

In our clinic, this plan, which was found to be successful in routine patient QA evaluation, achieved the best value in the use of cylindrical/inhomogeneous phantom using the 3%/1mm (94.25). According to the 3%/2 mm criterion we evaluated in the clinic, Setup 1 allowed treatment with 98.76%, whereas this value was

Table 2 The results of the gamma evaluation of the measured values by MatriXX and calculated differences % between reference values (99.5%) and obtained values at different grid sizes

Grid size (cm)	DD%/DTA mm	Setup 1	Setup 2	Reference criteria 3% 3 mm
0.2	3%/2 mm	98.76	88.39	99.5
	The Difference with Reference %	0.74	11.17	
	3%/1 mm	94.72	84.15	
	The Difference with Reference %	4.80	15.43	
0.1	3%/2 mm	98.26	91.46	
	The Difference with Reference %	1.25	8.08	
	3%/1 mm	94.25	89.35	
	The Difference with Reference %	5.28	10.20	

below our acceptance limit with 88.39% for Setup 2. The percentage differences of the other gamma values according to the reference value were calculated and given in Table 2.

Discussion

This section has been devoted to answering the questions posed in the previous sections.

1. What is the effect of the calculation grid size value selected in TPS on MU?

The MU and segment sizes significantly affect radiotherapy quality, as well as cancer risk that may arise from radiation therapy [24-27], which is also effective in the development of secondary cancer with an increase in MU.[28,29] In a plan equivalent to the human body with an inhomogeneous structure, Park et al. found the increase in MU with grid size change, 1% for 0.3 cm and 2% for 0.4 cm.[21]

In our study, when the 0.2 cm grid size for Setup 1, including square/homogenous phantom, was taken as a reference grid size, the MU values for 0.3 cm and 0.1 cm increased by 0.09% and 0.22%, respectively. For Setup 2 containing cylindrical/inhomogeneous phantoms, MU values for 0.1cm increased by 0.12%, and decreased by 0.15% for 0.3 cm. In the evaluation for critical organs, Dempsey et al. also reported that when the higher grid size was studied, MU would be more likely to cause overdose, especially in series and critical organs, and the planned target volume would provide lower coverage.[19]

2. What is the effect of the selected Grid Size value in the TPS on 2D array gamma evaluation and absorbed dose measurements?

IMRT plans calculated in large grid sizes show lower doses in high gradient dose regions.[30] In our study, similar results were found for ion chamber placement, which is known to coincide with the high gradient dose region. The findings showed that there are differences in the grid size selection in the assessment of calculated-measured dose differences per field and dose difference assessment for the total field. This may be a separate research topic, and all CD-MD differences in Setup 1 appear to be within limits (<3%). In Setup 2, the dose differences for all grid size calculations, results are within acceptable limits (<3%) except the Q1 field. The distance between MatriXX detectors is 0.762 cm. Therefore, the software interpolates existing doses at intermediate values. In the Niemierko and Goitein's studies, the grid evaluated the accuracy of interpolated doses using a Fermi function that provides a one-dimensional high-gradient dose profile for linear interpolation and beam penumbra according to size.[17] The beam penumbra region showed a steeper dose drop due to lateral electron disequilibrium when small fields were irradiated.[31] Therefore, the use of large grid sizes in high-dose gradient regions will increase the error even more since electron disequilibrium is more effective, especially in small fields.

Our clinical standard is to establish the patient plans calculated in the 0.2 cm grid size and the QA plan with 0.1 cm and to perform gamma evaluation according to the 3%/3mm criteria after measurement. For grid sizes used in this study, the best results for all three evaluation criteria in Setup 1 were found in grid size 0.2. For Setup 2, the grid sizes give us more concordance between CD-MD and the results in 0.1.

3. What is the effect of using different DTA values on gamma results in 2D array measurements?

Pathak et al. found that the 5%/5 mm evaluation criteria exceed 95% of all grid size calculations. In the same study, it was reported that as the DTA shrinks, the passing rate falls below 90%.[13] In our study, when we look at the differences according to the reference gamma pass value in Table 2, this value decreases

Turk J Oncol 2020;35(3):298–305
doi: 10.5505/tjo.2020.2264

as DTA decreases for both setup and all grid sizes and increases the difference with the reference value. The largest difference for Setup 1 and Setup 2 was found to be 5.28% and 15.43%, respectively, at grid size 0.1 cm and 0.2 cm for 1mm DTA.

4. What is the effect of using cylindrical/inhomogeneous (C/I) phantom instead of square/homogeneous (S/H) phantom in 2D array gamma evaluation and absorbed dose measurements?

For absorbed dose measurements with ion chamber and TPS absorbed dose calculations, when the Setup 1 and Setup 2 were compared, the most appropriate grid for the measurements with S/H phantom was found to be 0.3 cm and 0.2 cm for Setup 2. The biggest differences in grid size were found to be 1% for 0.3 cm and 1.52% for 0.2 cm. This shows the effects of inhomogeneous environment and cylindrical phantom on the dose change in absorbed dose measurements.

In the literature, a study with clear information on dosimetric comparisons of C/I phantoms used for patient QA uptake and S/H phantoms used for standard QA uptake, to our knowledge, was not available. In this study, the environment was transformed into a C/I structure, and values below the acceptance gamma criteria were encountered.

There are nine inserts of different density in the phantom, which contains inhomogeneous structure. The behavior of photons in a medium of homogeneous density is not the same in environments with different densities. The reasons for this are photon interactions with materials with different components, mass reduction coefficient, effective atomic number and electron density parameters. The mass reduction coefficient (μ/ρ) is a measure of the number of photons that interact (scatter/absorber) with the target material. When a photon beam passes through the material and interacts, the photons are either absorbed (photoelectric effect, double and triple formation, photonuclear) or scattered (coherent and incoherent scattering).[32] Water equivalent solid even though the dominant phenomenon in homogeneous phantom is again the incoherent scattering when the photon beam becomes a bone structure, it is seen that the coherent scattering increases compared to water, and especially the photoelectric event increases more than five times. In the same way, nuclear pairing increased, and electron pairing decreased.

Conclusion

A setup where both the ion chamber and MatriXX were used simultaneously in the patient QA test before treatment with IMRT was proposed in this study. The use of this setup will save time for the medical physicist. Moreover, the gamma evaluation results changed significantly using C/I phantoms containing inhomogeneous structures in place of routinely used the S/H phantoms. While the grid size was 0.2 in Setup 2, the decrease rate in gamma evaluation was found higher than 0.1 grid size value. In absorbed dose comparisons, the differences between homogeneous and inhomogeneous phantom were found to be less than 3%.

Peer-review: Externally peer-reviewed.

Conflict of Interest: None declared.

Ethics Committee Approval: This study was conducted in accordance with local ethical rules.

Financial Support: None declared.

Authorship contributions: Concept – A.İ.; Design – A.İ., İ.H.S.; Supervision – A.İ., İ.H.S.; Funding – None; Materials – A.İ., İ.H.S.; Data collection and/or processing – A.İ.; Data analysis and/or interpretation – A.İ., İ.H.S.; Literature search – A.İ, İ.H.S., R.Ü.; Writing – A.İ., İ.H.S., R.Ü.; Critical review – A.İ., İ.H.S., R.Ü.

References

1. Portelance L, Chao KS, Grigsby PW, Bennet H, Low D. Intensity-modulated radiation therapy (IMRT) reduces small bowel, rectum, and bladder doses in patients with cervical cancer receiving pelvic and para-aortic irradiation. Int J Radiat Oncol Biol Phys 2001;51(1):261–6.
2. Bayouth JE, Wendt D, Morrill SM. MLC quality assurance techniques for IMRT applications. Med Phys 2003;30(5):743–50.
3. Chui CS, Spirou S, LoSasso T. Testing of dynamic multileaf collimation. Med Phys 1996;23(5):635–41.
4. LoSasso T, Chui CS, Ling CC. Comprehensive quality assurance for the delivery of intensity modulated radiotherapy with a multileaf collimator used in the dynamic mode. Med Phys 2001;28(11):2209–19.
5. Gopi S, Ganesan S, Aruna P, Bouchaib R, Supe SS. Influence of photon beam energy on IMRT plan quality for radiotherapy of prostate cancer. Rep Pract Oncol Radiother 2009;14(1):18–31.
6. Bhardwaj AK, Sharma SC, Rana B, Shukla A. Study of 2D ion chamber array for angular response and QA of dynamic MLC and pretreatment IMRT plans. Rep Pract Oncol Radiother 2009;14(3):89–94.
7. Winiecki J, Morgas T, Majewska K, Drzewiecka B. The gamma evaluation method as a routine QA procedure of IMRT. Rep Pract Oncol Radiother 2009;14(5):162–8.

8. Slosarek K, Szlag M, Bekman B, Grzadziel A. EPID in vivo dosimetry in RapidArc technique. Rep Pract Oncol Radiother 2010;15(1):8–14.
9. Stock M, Kroupa B, Georg D. Interpretation and evaluation of the gamma index and the gamma index angle for the verification of IMRT hybrid plans. Phys Med Biol 2005;50(3):399–411.
10. Wiezorek T, Banz N, Schwedas M, Scheithauer M, Salz H, Georg D, et al. Dosimetric quality assurance for intensity-modulated radiotherapy feasibility study for a filmless approach. Strahlenther Onkol 2005;181(7):468–74.
11. Alber M, Broggi S, Wagter CD, Eichwurzel I, Engstrom P, Fiorino C, et al. Guidelines for the verification of IMRT. Brussels, Belgium: ESTRO; 2008.
12. Ezzell GA, Burmeister JW, Dogan N, LoSasso TJ, Mechalakos JG, Mihailidis D, et al. IMRT commissioning: multiple institution planning and dosimetry comparisons, a report from AAPM Task Group 119. Med Phys 2009;36(11):5359–73.
13. Pathak P, Mishra PK, Birbiya N. Dosimetric Study on Variations of Gamma Index (GI) in Pre-Treatment Verification Procedure in Intensity Modulated Radiotherapy (IMRT) Plans with Varying Grid Sizes Using 2D Array Detectors. J Cancer Sci Ther 2015;7:161–6.
14. Low DA, Moran JM, Dempsey JF, Dong L, Oldham M. Dosimetry tools and techniques for IMRT. Med Phys 2011;38(3):1313–38.
15. Van Esch A, Bohsung J, Sorvari P, Tenhunen M, Paiusco M, Iori M, et al. Acceptance tests and quality control (QC) procedures for the clinical implementation of intensity modulated radiotherapy (IMRT) using inverse planning and the sliding window technique: experience from five radiotherapy departments. Radiother Oncol. 2002;65(1):53–70.
16. Jursinic PA, Nelms BE. A 2-D diode array and analysis software for verification of intensity modulated radiation therapy delivery. Med Phys 2003;30(5):870–9.
17. Niemierko A, Goitein M. The influence of the size of the grid used for dose calculation on the accuracy of dose estimation. Med Phys 1989;16(2):239–47.
18. Feygelman V, Zhang G, Stevens C. Initial dosimetric evaluation of SmartArc - a novel VMAT treatment planning module implemented in a multi-vendor delivery chain. J Appl Clin Med Phys 2010;11(1):3169.
19. Dempsey JF, Romeijn HE, Li JG, Low DA, Palta JR. A fourier analysis of the dose grid resolution required for accurate IMRT fluence map optimization. Med Phys 2005;32(2):380–8.
20. Chung H, Jin H, Palta J, Suh TS, Kim S. Dose variations with varying calculation grid size in head and neck IMRT. Phys Med Biol 2006;51(19):4841–56.
21. Park JY, Kim S, Park HJ, Lee JW, Kim YS, Suh TS. Optimal set of grid size and angular increment for practical dose calculation using the dynamic conformal arc technique: a systematic evaluation of the dosimetric effects in lung stereotactic body radiation therapy. Radiat Oncol 2014;9:5.
22. De Martin E, Fiorino C, Broggi S, Longobardi B, Pierelli A, Perna L, et al. Agreement criteria between expected and measured field fluences in IMRT of head and neck cancer: the importance and use of the gamma histograms statistical analysis. Radiother Oncol 2007;85(3):399–406.
23. Pulliam KB, Followill D, Court L, Dong L, Gillin M, Prado K, et al. A six-year review of more than 13,000 patient-specific IMRT QA results from 13 different treatment sites. J Appl Clin Med Phys 2014;15(5):4935.
24. Shaw E, Scott C, Souhami L, Dinapoli R, Kline R, Loeffler J, et al. Single dose radiosurgical treatment of recurrent previously irradiated primary brain tumors and brain metastases: final report of RTOG protocol 90-05. Int J Radiat Oncol Biol Phys 2000;47(2):291–8.
25. Feuvret L, Noël G, Mazeron JJ, Bey P. Conformity index: a review. Int J Radiat Oncol Biol Phys 2006;64(2):333–42.
26. Galvin JM, Ezzell G, Eisbrauch A, Yu C, Butler B, Xiao Y, et al. Implementing IMRT in clinical practice: a joint document of the American Society for Therapeutic Radiology and Oncology and the American Association of Physicists in Medicine. Int J Radiat Oncol Biol Phys 2004;58(5):1616–34.
27. Lee MT, Purdie TG, Eccles CL, Sharpe MB, Dawson LA. Comparison of simple and complex liver intensity modulated radiotherapy. Radiat Oncol 2010;5:115.
28. Hall EJ, Wuu CS. Radiation-induced second cancers: the impact of 3D-CRT and IMRT. Int J Radiat Oncol Biol Phys 2003;56(1):83–8.
29. Kry SF, Salehpour M, Followill DS, Stovall M, Kuban DA, White RA, et al. The calculated risk of fatal secondary malignancies from intensity-modulated radiation therapy. Int J Radiat Oncol Biol Phys 2005;62(4):1195–203.
30. Videtic GM, Hu C, Singh AK, Chang JY, Parker W, Olivier KR, et al. A Randomized Phase 2 Study Comparing 2 Stereotactic Body Radiation Therapy Schedules for Medically Inoperable Patients With Stage I Peripheral Non-Small Cell Lung Cancer: NRG Oncology RTOG 0915 (NCCTG N0927). Int J Radiat Oncol Biol Phys 2015;93(4):757–64.
31. Carrasco P, Jornet N, Duch MA, Weber L, Ginjaume M, Eudaldo T, et al. Comparison of dose calculation algorithms in phantoms with lung equivalent heterogeneities under conditions of lateral electronic disequilibrium. Med Phys 2004;31(10):2899–911.
32. Manjunatha HC. A study of photon interaction parameters in lung tissue substitutes. J Med Phys 2014;39(2):112–5.